AGU PUBLICATIONS

Geophysical Research Letters

RESEARCH LETTER
10.1002/2016GL068303

Key Points:
- The AMO does not result solely from oceanic processes
- Clouds and anomalous net surface radiation covary with the AMOC
- Cloud feedback is necessary for the tropical portion of the AMO

Supporting Information:
- Supporting Information S1

Correspondence to:
P. T. Brown,
Patrick.Brown@duke.edu

Citation:
Brown, P. T., M. S. Lozier, R. Zhang, and W. Li (2016), The necessity of cloud feedback for a basin-scale Atlantic Multidecadal Oscillation, *Geophys. Res. Lett.*, *43*, 3955–3963, doi:10.1002/2016GL068303.

Received 16 FEB 2016
Accepted 1 APR 2016
Accepted article online 5 APR 2016
Published online 30 APR 2016

The necessity of cloud feedback for a basin-scale Atlantic Multidecadal Oscillation

Patrick T. Brown[1], M. Susan Lozier[1], Rong Zhang[2], and Wenhong Li[1]

[1]Earth and Ocean Sciences, Nicholas School of the Environment, Duke University, Durham, North Carolina, USA, [2]National Oceanic and Atmospheric Administration, Geophysical Fluid Dynamics Laboratory, Princeton, New Jersey, USA

Abstract The Atlantic Multidecadal Oscillation (AMO), characterized by basin-scale multidecadal variability in North Atlantic sea surface temperatures (SSTs), has traditionally been interpreted as the surface signature of variability in oceanic heat convergence (OHC) associated with the Atlantic Meridional Overturning Circulation (AMOC). This view has been challenged by recent studies that show that AMOC variability is not simultaneously meridionally coherent over the North Atlantic and that AMOC-induced low-frequency variability of OHC is weak in the tropical North Atlantic. Here we present modeling evidence that the AMO-related SST variability over the extratropical North Atlantic results directly from anomalous OHC associated with the AMOC but that the emergence of the coherent multidecadal SST variability over the tropical North Atlantic requires cloud feedback. Our study identifies atmospheric processes as a necessary component for the existence of a basin-scale AMO, thus amending the canonical view that the AMOC-AMO connection is solely attributable to oceanic processes.

1. Introduction

The Atlantic Multidecadal Oscillation (AMO) [*Enfield et al.*, 2001] is second only to the El Niño–Southern Oscillation in terms of its contribution to global sea surface temperature (SST) variability over the observational record [*Messié and Chavez*, 2011]. As such, the AMO has been implicated as a strong influence on several aspects of global climate such as Atlantic hurricane activity [*Goldenberg et al.*, 2001; *Knight et al.*, 2006; *Zhang and Delworth*, 2006], North American and European climate [*Enfield et al.*, 2001; *Sutton and Hodson*, 2005], Sahel and Amazonian rainfall [*Folland et al.*, 1986; *Knight et al.*, 2006; *Martin et al.*, 2014], Arctic sea ice extent [*Mahajan et al.*, 2011; *Zhang*, 2015], and even global mean temperature [*Brown et al.*, 2015a; *Chylek et al.*, 2014; *Schlesinger and Ramankutty*, 1994]. While the AMO's far-reaching influence on the climate system is well appreciated, the fundamental physics of the AMO remain uncertain and a matter of debate.

Current physical explanations for the AMO differ in several aspects, but most rest on the underlying premise that the AMO is the proximate result of interdecadal variability in the strength of the Atlantic Meridional Overturning Circulation (AMOC) [*Ba et al.*, 2014; *Delworth and Mann*, 2000; *Knight et al.*, 2005; *McCarthy et al.*, 2015; *Medhaug and Furevik*, 2011]. AMOC variability itself is often attributed to changes in North Atlantic Deep Water (NADW) formation due to anomalous Arctic freshwater fluxes [*Jungclaus et al.*, 2005] and/or atmospheric modes such as the North Atlantic Oscillation [*Buckley and Marshall*, 2016; *Latif et al.*, 2006; *Latif and Keenlyside*, 2011; *Li et al.*, 2013; *Sun et al.*, 2015]. Despite the indirect role for the atmosphere, the physical connection between the AMOC and the AMO is typically described in terms of oceanic processes alone: since the AMOC transports heat northward over the entire Atlantic, an increase in NADW formation should increase the strength of the AMOC, thus increasing oceanic meridional heat transport (MHT) convergence in the North Atlantic, resulting in a basin-scale warming of SSTs [*Knight et al.*, 2005].

A challenge to this canonical view has recently materialized, as several studies have suggested that AMOC variability is not simultaneously meridionally coherent across the entire North Atlantic [*Bingham et al.*, 2007; *Lozier*, 2010, 2012; *Lozier et al.*, 2010]. Additionally, *Zhang and Zhang* [2015] showed that the AMOC-induced convergence of MHT anomalies is much weaker in the tropical North Atlantic (TNA; defined here as the Atlantic between the equator and 34°N) than it is in the extratropical North Atlantic (ENA; defined here as the Atlantic between 34°N and 65°N), suggesting that a mechanism other than direct AMOC-induced changes in MHT convergence is required for linking the AMOC variability at northern high latitudes with the emergence of a basin-scale AMO. Below we present modeling evidence that the cloud feedback is a crucial component of this mechanism.

2. Methods and Definitions

Uncovering the physical explanation for the AMO has been a challenge due to the short observational record relative to its characteristic time scale [*Ting et al*., 2009], the uncertain influence of externally forced versus internally generated SST variability over the observational record [*Booth et al*., 2012; *Brown et al*., 2015b; *Zhang et al*., 2013], difficulty in the quantification of surface and top-of-atmosphere energy fluxes over the observational record [*Trenberth et al*., 2009], and the lack of any direct AMOC observations until relatively recently [*Cunningham et al*., 2007; *Rayner et al*., 2011]. Considering these challenges, it has been fruitful to study the physics underlying the AMO in unforced control runs of coupled general circulation models (CGCMs) and we adopt that strategy here.

2.1. Coupled Model Intercomparison Project Phase 5 and Geophysical Fluid Dynamics Laboratory CM2.1 Control Runs

We utilized 15 unforced CGCM control runs from the Coupled Model Intercomparison Project Phase 5 (CMIP5) archive [*Taylor et al*., 2011] and an unforced Geophysical Fluid Dynamics Laboratory (GFDL) CM2.1 run [*Delworth et al*., 2006], in which external radiative forcings were held constant and thus all variability emerged spontaneously from the internal dynamics of the modeled climate system. Analysis was conducted on the first 200 years of each CGCM's control run. We only analyzed CGCMs with a global-mean, time-mean net top-of-atmosphere (TOA) energy imbalance of less than 2 W/m^2 so that we could focus our analysis on CGCMs that were not experiencing excessive drift.

2.2. GFDL CM2.1 Control Run Without Cloud Feedback

In the analysis below we utilize a GFDL CM2.1 control run without cloud feedback. This experiment was identical to the fully coupled GFDL CM2.1 run, except that the three prognostic cloud properties (total cloud liquid in each grid box, total cloud ice in each grid box, and the fraction of each grid box covered by cloud) were prescribed over the global domain at each time step and repeated for each year of the simulation. These prescribed cloud properties came from one arbitrary year in the GFDL CM2.1 unforced simulation but were adjusted to have the same climatological monthly means as the GFDL CM2.1 run with cloud feedback so that the simulated ocean and atmosphere climatology was similar in both runs. See *Zhang et al*. [2010] for further details on the experiment.

2.3. Data Preprocessing

All CMIP5 output were regridded from each CGCM's native grid to a common $2° \times 2°$ grid via bilinear interpolation so that values could be compared at the same locations. All time series were anomalized by subtracting the climatological mean of the variable from each year in the time series. Additionally, all time series were linearly detrended so that any remaining model drift was discarded. Figures 2a–2c show the periodogram for unsmoothed annual time series, but all other time series were smoothed with a 15 year Lowess [*Cleveland*, 1979] filter prior to subsequent analysis so that the interdecadal component of variability could be investigated. Conclusions of this study are robust to smoothing at the 30 year time scale (not shown).

2.4. AMO Index

We define the AMO as the low-pass filtered (15 year Lowess [*Cleveland*, 1979]) spatially weighed mean SST from 7.5°W to 75°W and 0°N to 65°N over the Atlantic Ocean. The AMO indices for each CGCM investigated are shown in Figures S1 and S9 in the supporting information.

2.5. AMOC Index

The strength of the AMOC in the two GFDL CM2.1 experiments was approximated as the low-pass filtered time series (15 year Lowess [*Cleveland*, 1979]) of the maximum zonally integrated Atlantic meridional overturning stream function at 45°N in density space. The AMOC indices are shown in Figure S9 in the supporting information. Similar results are obtained when the AMOC index was defined at 26°N (see Figure S13 in the supporting information).

2.6. Meridional Heat Transport and Meridional Heat Transport Convergence

The meridional heat transport (MHT) was defined as the zonally integrated northward heat transport across the entire Atlantic at each latitude, and the MHT convergence was defined as the negative of the latitudinally weighed meridional derivative of the MHT.

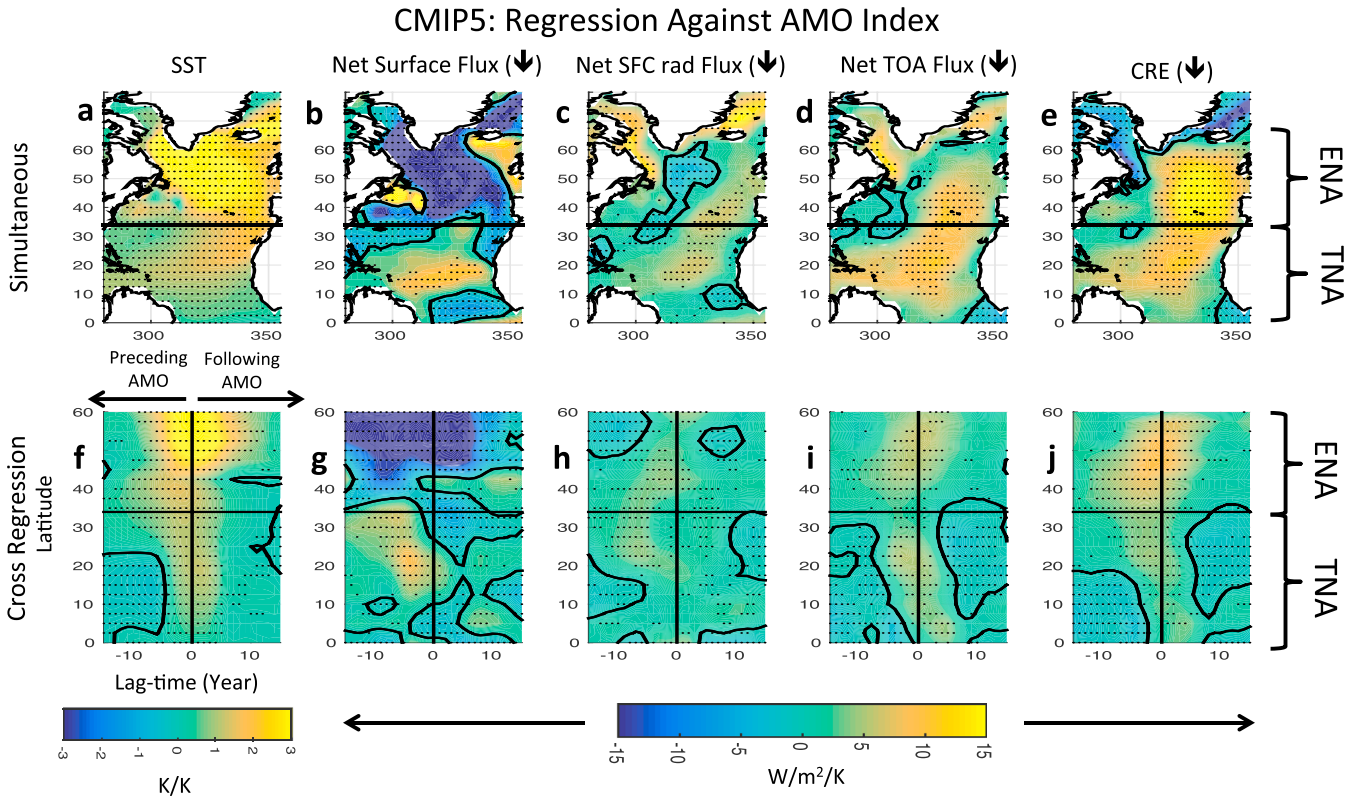

Figure 1. Spatiotemporal structure of SST, surface (SFC), and top-of-atmosphere (TOA) energy flux anomalies associated with the AMO in CMIP5 unforced control runs. Plotted are the multimodel means of the least squares linear regression coefficient between the labeled variable and the AMO index. (a–e) The simultaneous regression with the AMO index and (f–j) the cross regression of the North Atlantic zonal mean time series with the AMO index. All energy fluxes are positive downward. Stippling represents where over 80% of the CGCMs agree on the sign of the regression coefficient. Note, however, that CGCMs from the CMIP5 ensemble cannot be considered to be independent [*Knutti et al.*, 2013]. Figures S2–S6 in the supporting information show spatial plots for each individual CMIP5 CGCM used. Note that while zonal mean plots reflect the basin-scale features, they can also obscure small-scale features (apparent in the maps) that might be locally important.

2.7. Use of Cloud Radiative Effect

Below we utilize the change in cloud radiative effect (CRE) with SST to investigate the radiative impact of cloud variability. The CRE is a measure of the impact of clouds on the radiation budget relative to a cloudless atmosphere [*Ramanathan et al.*, 1989]. Thus, a change in the CRE with SST is not a direct measure of cloud feedback since CRE changes can results from a change in cloud properties *or* a change in the clear-sky radiation budget [*Soden et al.*, 2004], leaving some ambiguity for the cloud effect over regions with large changes in the clear-sky energy budget.

3. Heat Flux and the AMO in CGCMs

We first examine the structure of the AMO and its associated anomalous heat flux in output from a number of CGCMs that participated in CMIP5. We focus on multimodel mean relationships in order to emphasize features that are robust across the ensemble, but results from individual models are shown in Figures S1–S6 in the supporting information. Our analysis confirms that CGCMs tend to simulate a basin-scale AMO with simultaneously coherent interdecadal SST variability between the ENA and the TNA (Figures 1a and 1f) [*Ba et al.*, 2014]. CGCMs indicate that the positive phase of the AMO is associated with anomalous negative (i.e., upward) net surface heat flux over large portions of the ENA, in conjunction with the AMO (Figure 1b) and preceding the AMO peak for several years (Figures 1g and S7b in the supporting information). On the contrary, the AMO positive phase is associated with substantial areas of anomalously positive (i.e., downward) net surface heat flux over the TNA, in conjunction with the AMO (Figure 1b) and preceding the AMO peak for several years (Figures 1g and S7b in the supporting information). These contrasting relationships indicate that over the ENA, the anomalous net surface heat flux tends to *damp* the AMO-related interdecadal

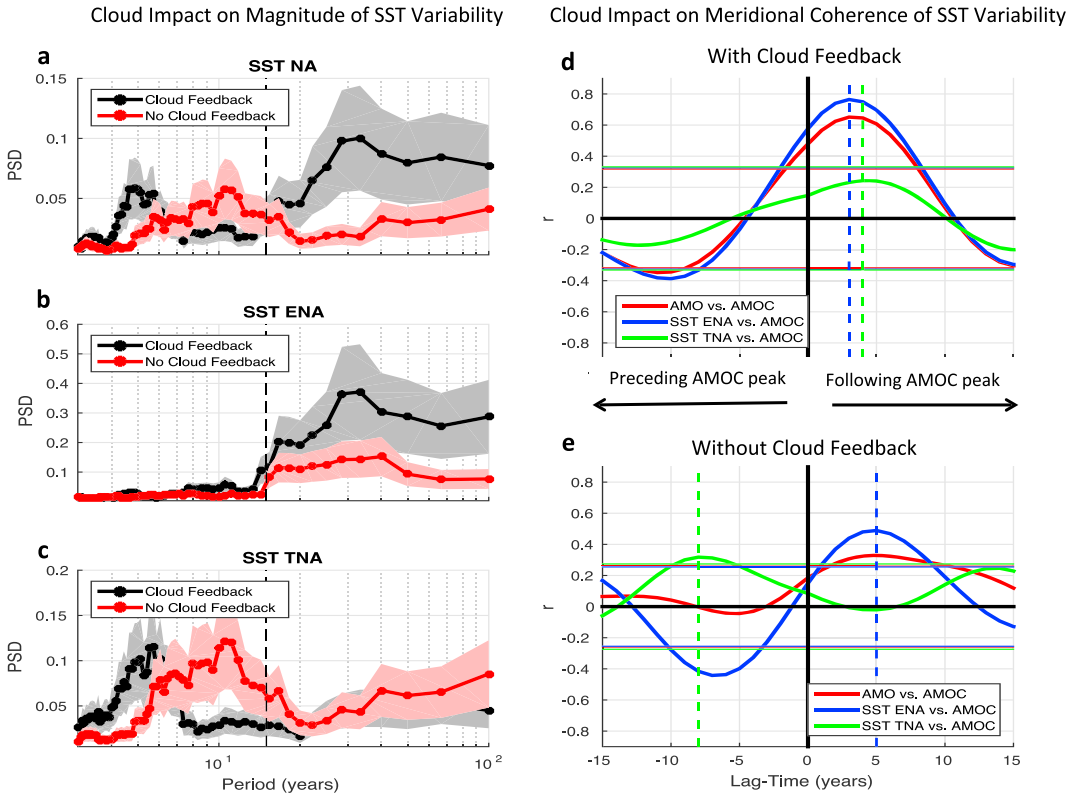

Figure 2. SST variability and its meridional coherence with and without cloud feedback in GFDL CM2.1. (a) Power spectral density of the North Atlantic SST (0–65°N) in the model configuration with (black line) and without (red line) cloud feedback. (b) Same as in Figure 2a but applied to SSTs over the ENA. (c) Same as in Figure 2a but applied to SSTs over the TNA. The power spectral density curves are smoothed with a nine-period running mean [*von Storch and Zwiers*, 2003]. (d) Cross correlation between the AMOC index and SSTs over different domains in the North Atlantic in the model with cloud feedback. (e) Same as in Figure 2d but in the model without cloud feedback. The vertical dashed lines in Figures 2a–2c demark the 15 year time scale where time series were smoothed prior to the calculations shown in Figures 2d and 2e. In Figures 2d and 2e, vertical dashed lines indicate the time lag of maximum correlation. Note that the maximum correlation between the AMOC and TNA SST in the no cloud feedback case occurs at −8 years because without cloud feedback, ENA and TNA SSTs are out of phase, and thus, positive TNA SSTs occur during the previous iteration of the cycle. In Figures 2d and 2e the error ranges mark the 5th and 95th significance levels (as calculated via a Monte Carlo method, see supporting information). The time series underlying these plots are shown in Figure S9 in the supporting information.

SST variability [*Gulev et al.*, 2013; *O'Reilly et al.*, 2016], while over the TNA, the anomalous net surface heat flux tends to *enhance* the AMO-related interdecadal SST variability. Note that the amplitude of the anomalous net surface heat flux is much smaller over the TNA than that over the ENA (Figures 1b and 1g). Additionally, Figures S7a and S7b in the supporting information indicate that over most of the TNA, the net surface heat flux contributes to the SST tendency associated with the AMO, while net surface heat flux tends to oppose the SST tendency associated with the AMO over large portions of the ENA.

An examination of the anomalous TOA radiative flux associated with the AMO (Figures 1d and 1i) indicates that changes in radiatively active constituents of the atmosphere result in anomalous surface radiative fluxes (Figures 1c and 1h) that enhance AMO magnitude and variability over large portions of both the ENA and the TNA. The importance of cloud feedback has previously been identified for unforced Atlantic SST variability [*Bellomo et al.*, 2015; *Evan et al.*, 2012; *Yuan et al.*, 2016], as well as for the Atlantic SST response to an abrupt AMOC weakening [*Zhang et al.*, 2010]. Furthermore, cloud feedback associated with local unforced surface temperature variability have been shown to be positive over the majority of the world's oceans [*Brown et al.*, 2016]. These studies lead us to suspect that clouds might play a role in modulating heat flux variability associated with the AMO. Indeed, the spatial pattern of the anomalous CRE over much of the North Atlantic (Figures 1e and 1j) indicates that changes in clouds have a positive feedback on AMO variability over most of the basin in CMIP5 models. Decomposition of the radiation budget reveals that the

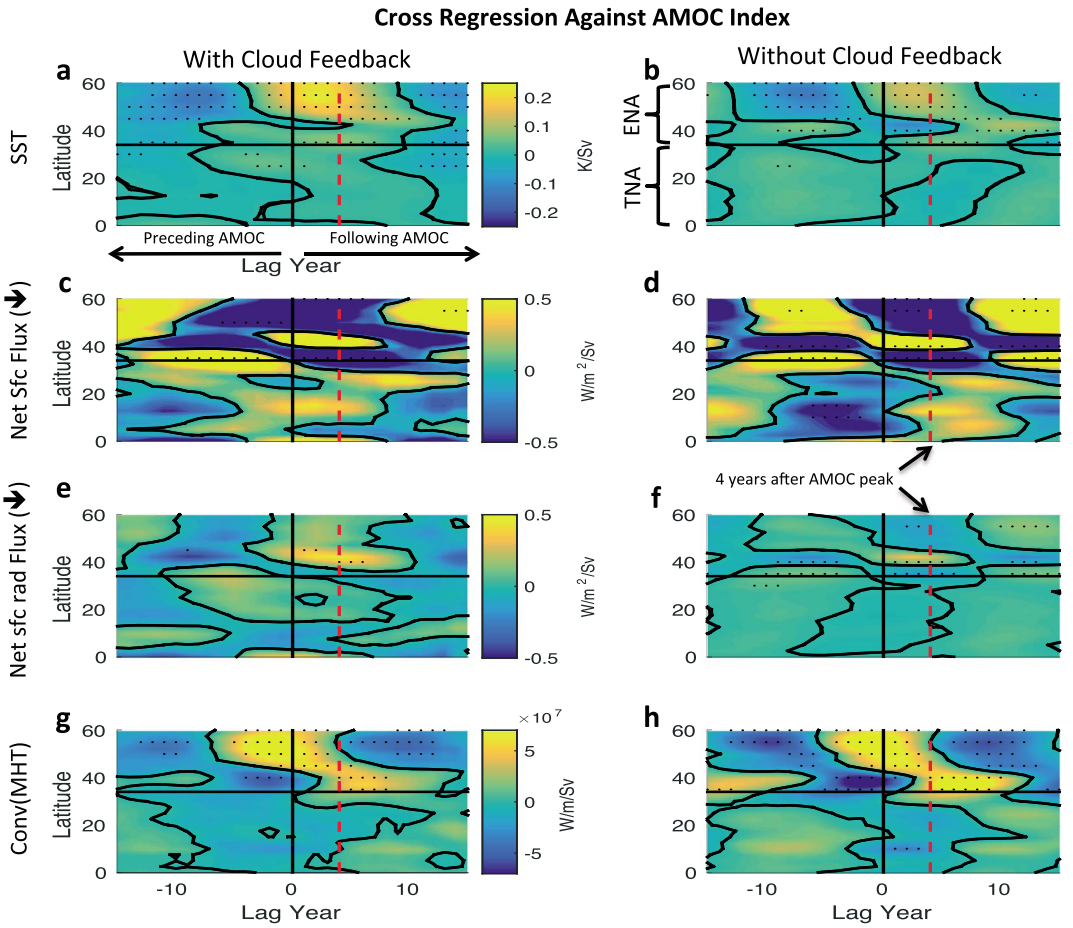

Figure 3. Impact of cloud feedback on SST and surface heat flux anomalies associated with AMOC variability. (a, c, e, and g) Least squares cross-regression coefficients between zonal mean time series of the labeled variable over the North Atlantic and the AMOC index in the GFDL CM2.1 model with cloud feedback. (b, d, f, and h) Same as in Figures 3a, 3c, 3e, and 3g but in the model without cloud feedback. Note that the AMOC variability itself is largely unaffected by cloud feedback (Figure S11 in the supporting information). All energy fluxes are positive downward. Stippling represents statistical significance using a Monte Carlo technique (see supporting information). The horizontal solid line separates the ENA from the TNA. Conclusions are not sensitive to the latitude where the AMOC index is defined (Figure S13 in the supporting information).

cloud components (Figures S8c, S8g, S8d, and S8h in the supporting information) play a leading role but that there are also amplifying effects in the clear-sky portion of the budget, both in the longwave, presumably via water vapor feedback (Figures S8a and S8e in the supporting information), and in the shortwave, presumably via sea ice feedback (Figure S8b and S8f in the supporting information).

4. The Necessity of Cloud Feedback for a Basin-Scale AMO

To quantify the impact of cloud feedback on the AMO, we compare the relationship between the AMOC, heat fluxes, and SSTs in a fully coupled control simulation of GFDL CM2.1 (henceforth referred to as the run "with cloud feedback") to the relationship in a GFDL CM2.1 simulation without a multiyear cloud feedback (henceforth referred to as the run "without cloud feedback"). See section 2 for more details.

A comparison of the two simulations reveals that cloud feedback greatly enhances the magnitude of interdecadal North Atlantic SST variability (Figure 2a), as well as interdecadal SST variability over the ENA (Figure 2b). Cloud feedback does not cause a clear enhancement of interdecadal SST variability over the TNA (Figure 2c). However, the cloud feedback greatly enhances the meridional coherence of SST variability in the North Atlantic (cf. Figures 2d and 2e). Specifically, in the run with cloud feedback, ENA and TNA SST variability each lag AMOC variability by ~4 years, consistent with previous studies [*Ba et al.*, 2014;

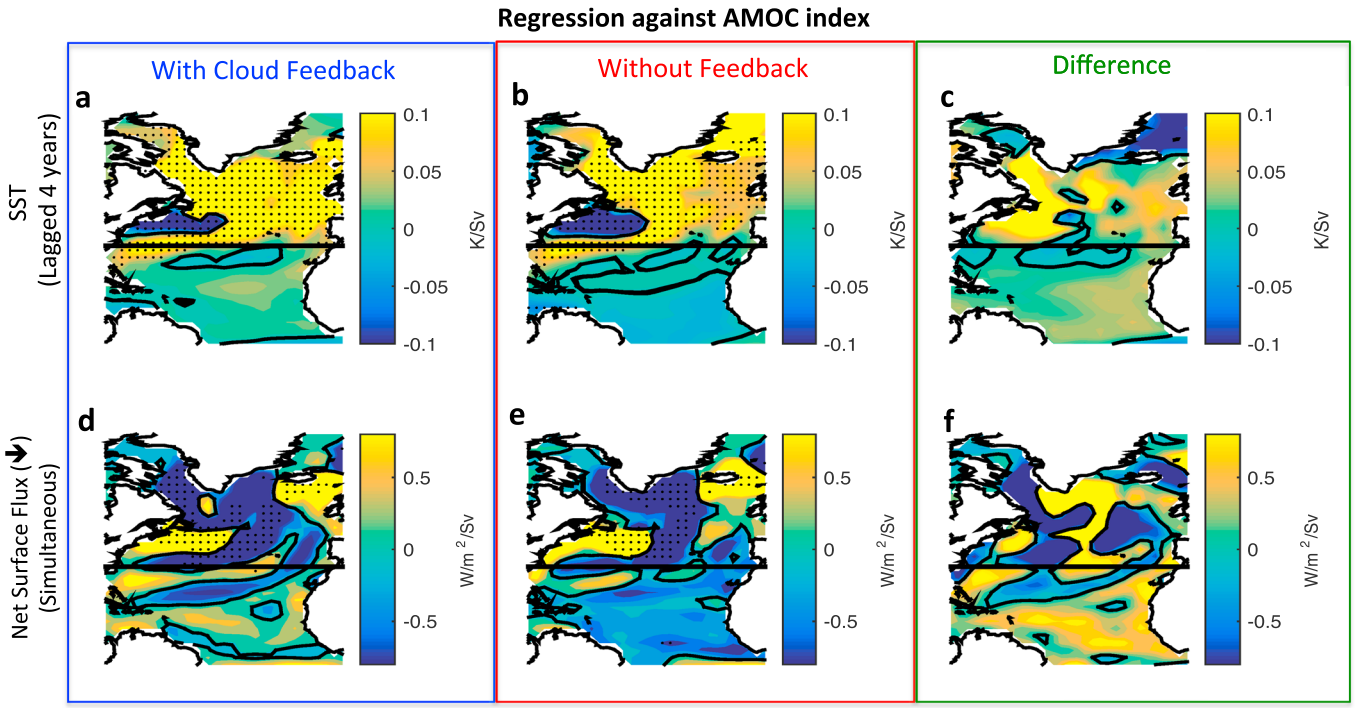

Figure 4. Least squares linear regression coefficient between the labeled variable and the AMOC index in the GFDL CM2.1 run with and without cloud feedback. (a–c) The regression coefficients are lagged 4 years because the AMO fully emerges 4 years after the AMOC peak (Figures 2d and 2e). (d–f) The regression coefficients are calculated simultaneous to the AMOC index so that their effect on the SST tendency is highlighted. For example, the negative net surface heat flux anomaly over the ENA in Figures 4d and 4e tends to damp the positive ENA SST anomaly in Figures 4a and 4b and is a response to the positive ocean heat transport convergence anomaly (Figures 3g and 3h). On the other hand, the positive net surface heat flux anomaly over the TNA in Figure 4d can be interpreted as contributing to the positive TNA SST anomaly 4 years later (Figure 4a). Stippling represents statistical significance using a Monte Carlo technique (see supporting information). Net surface energy fluxes are positive downward. Note that the AMOC variability itself is largely unaffected by cloud feedback (Figure S11 in the supporting information).

Zhang and Zhang, 2015]. Without cloud feedback, ENA SSTs still show significant correlation with the AMOC at a 4 year lag; however, the correlation between the AMOC and TNA SSTs at that lag drops to zero (Figure 2e). Thus, the enhanced AMO variability in the run with cloud feedback is attributed to the enhanced ENA SST variability (~54% increase in the low-frequency ENA SST standard deviation; Figure S10 in the supporting information) *and* to the enhanced coherence between ENA and TNA SST variabilities (see also Figure S12 in the supporting information and associated discussion).

Figures 3 and 4 illustrate how cloud feedback alters the relationship between the AMOC, North Atlantic SSTs, and surface energy fluxes. With cloud feedback, a positive AMOC anomaly is associated with anomalously positive SSTs over almost the entire North Atlantic ~4 years later (Figures 3a and 4a) except for the negative SST anomaly over the Gulf Stream region that emerges due to local oceanic meridional heat transport (MHT) divergence [*Zhang and Zhang*, 2015]. The source of heat for the positive SST anomalies over the northern ENA is mostly oceanic MHT convergence that persists from ~7 years prior to ~4 years following the AMOC maximum (Figure 3g). The net surface heat flux over the ENA tends to be negative both in conjunction with the AMOC (Figure 4d) and surrounding it in time for several years (Figure 3c), indicating surface damping of the SST anomalies over the ENA. The situation is quite different over the TNA where there tends to be a weak MHT *divergence* for ~10 years prior to and persisting for several years following the AMOC maximum (Figure 3g). Despite this MHT divergence, zonal mean TNA SST anomalies become positive at all latitudes ~4 years after the AMOC peak (Figures 3a and 4a), due to persistently positive net surface heat fluxes (Figure 3c and 4d). The anomalously positive net surface heat fluxes over the TNA are partially explained by anomalously positive net surface radiative flux (Figure 3e) but are also affected by positive turbulent energy fluxes, discussed further below.

The model run without cloud feedback shows an AMOC-SST-surface energy flux relationship that is fundamentally altered. ENA SSTs still vary due to MHT convergence (Figure 3h), but much of the TNA experiences

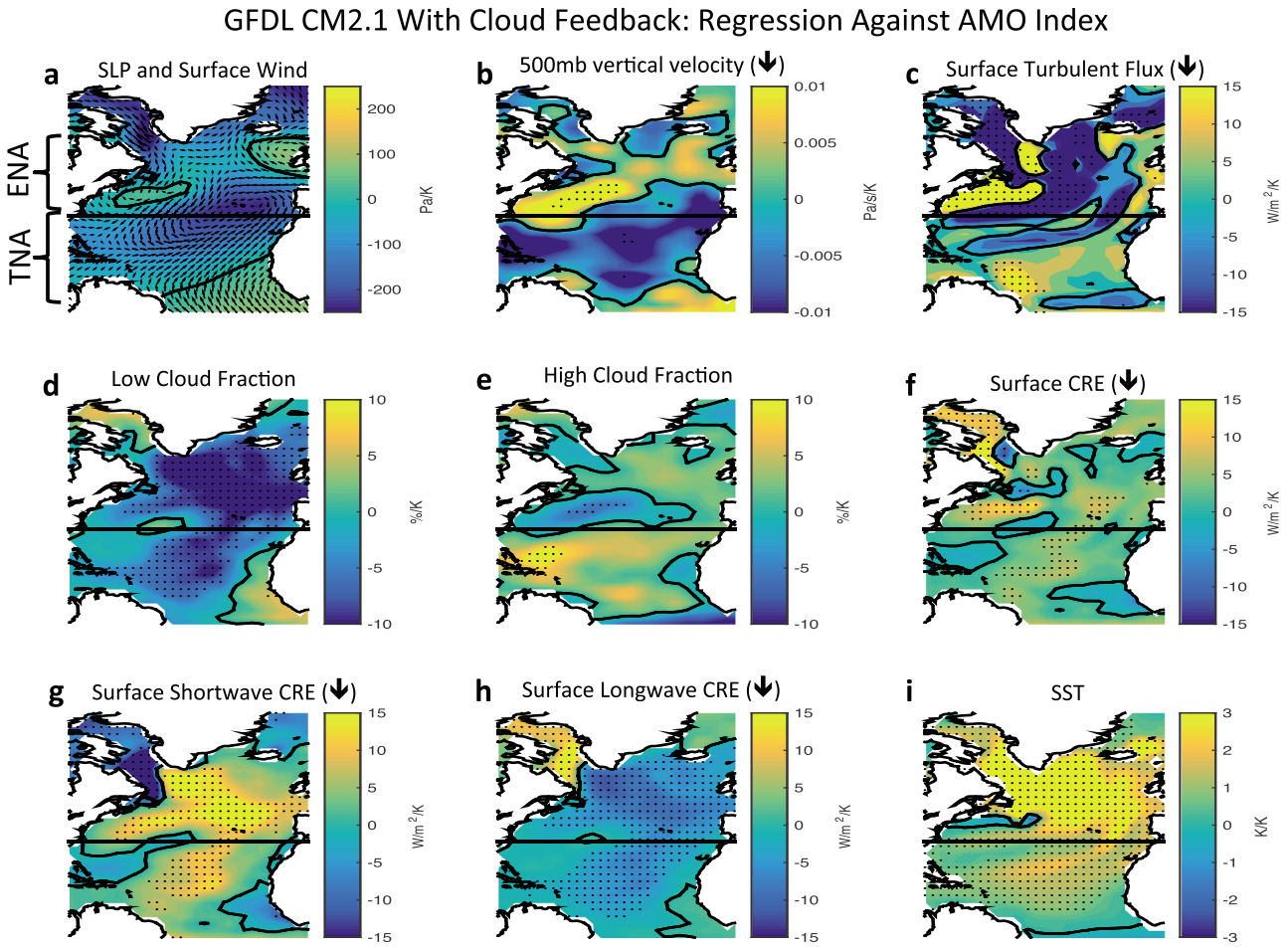

Figure 5. Least squares linear regression coefficient between the labeled variable and the AMO index in the GFDL CM2.1 run with cloud feedback. All energy fluxes are positive downward. Stippling represents statistical significance calculated using a Monte-Carlo technique (see supporting information).

anomalously *negative* SSTs ~4 years after the AMOC peak, producing a dipole pattern over the North Atlantic (Figures 3b and 4b). Contrary to the run with cloud feedback, the run without cloud feedback shows that from ~10 years prior to ~3 years after the AMOC peak, the net surface heat flux is mostly negative over the TNA (Figures 3d and 4e) contributing to the emergence of the negative SST anomaly there. Thus, the cloud feedback produces an enhancement of SST variation over the ENA and it reverses the sign of AMOC-induced SST variability (due to MHT divergence) over the TNA, allowing for the emergence of the basin-scale AMO (Figures 4a–4c).

5. Discussion and Conclusion

The apparent mechanisms responsible for the basin-scale AMO in the GFDL CM2.1 run with cloud feedback are summarized in Figure 5. A positive AMO is associated with a positive SST anomaly in the ENA (due to MHT convergence), which causes anomalously low sea level pressure (SLP) and anomalous cyclonic surface winds over the North Atlantic (Figure 5a) [*Yuan et al.*, 2016]. SSTs over the TNA warm partially because the anomalous cyclonic winds induced by the ENA SST anomaly weaken the northeasterly trades and induce anomalously positive turbulent heat fluxes (Figure 5c) in a manner similar to that described in the wind-evaporation-SST (WES) feedback [*Xie and Philander*, 1994]. Additionally, during positive AMO, the large-scale atmospheric response induces reduced low-level cloud fraction (Figure 5d), which may be associated with reduced atmospheric subsidence (Figure 5b) and thus reduced marine boundary layer inversion strength [*Myers and Norris*, 2013]. This reduction in low-cloud fraction produces compensating effects in the shortwave (Figure 5g) and

the longwave (Figure 5h) but results in an overall surface CRE response that is mostly positive over the basin (Figure 5f) [*Yuan et al*., 2016].

Thus, the cloud feedback directly induces a surface radiative heat flux response that enhances the AMO-related SST variability over most of the North Atlantic. This enhanced SST variability supports SLP and surface wind responses that are sufficiently large to produce an anomalously positive TNA turbulent heat flux (Figure 5c). In addition, the AMO-related SST variability over the TNA may be amplified by feedback involving SSTs and African dust [*Martin et al*., 2014; *Wang et al*., 2012; *Yuan et al*., 2016].

As mentioned above, atmospheric processes have previously been invoked as one of the physical explanations of NADW formation and thus AMOC variability [*Latif et al*., 2006; *Latif and Keenlyside*, 2011; *Li et al*., 2013; *Sun et al*., 2015]. However, AMOC variability has traditionally been linked to the AMO through oceanic processes alone. In contrast, it was recently suggested that the AMO in CGCMs might emerge without AMOC variability since slab ocean models produce similar AMO SST patterns and power spectra as CGCMs [*Clement et al*., 2015]. Our results indicate that AMOC variability is critical to the production of the AMO in CGCMs but that the AMOC-AMO connection is not solely attributable to oceanic processes. Specifically, we show that the ENA portion of the AMO is driven primarily by AMOC-induced OHC convergence but the cloud feedback provides a necessary teleconnection mechanism for the emergence of the coherent TNA portion of the AMO. This result is primarily based on an investigation of the effects of cloud feedback in a single CGCM (GFDL CM2.1), and thus, it would be valuable test this mechanism in other CGCMs.

Quantifying the cloud response to external forcing has long been recognized as a key path forward for narrowing the uncertainties in long-term projections of global warming. Our study supports the notion that cloud feedback mechanisms may also be crucial for the emergence of large-scale internal modes of variability [*Brown et al*., 2016, 2014]. Thus, progress toward understanding the role of clouds in the climate system should also improve our ability to predict regional and global climate on decadal time scales.

Acknowledgments

We thank Ming Zhao and Xiaosong Yang for their internal reviews and discussion of this work. We acknowledge the World Climate Research Programme's Working Group on Coupled Modelling, which is responsible for CMIP, and we thank the climate modeling groups for producing and making available their model output. For CMIP the U.S. Department of Energy's Program for Climate Model Diagnosis and Intercomparison provides coordinating support and led development of software infrastructure in partnership with the Global Organization for Earth System Science Portals. The CMIP5 data used for this study can be downloaded at http://cmip-pcmdi.llnl.gov/cmip5/data_portal.html, and the GFDL CM2.1 model output can be downloaded at http://data1.gfdl.noaa.gov/. Contact Patrick Brown (patrick.brown@duke.edu) for other data and code requests. This work was partially supported by NSF grants AGS-1147608 and OCE-1259102, as well as by the NIH grant NIH-1R21AG044294-01A1.

References

Ba, J., et al. (2014), A multi-model comparison of Atlantic multidecadal variability, *Clim. Dyn.*, *43*, 2333–2348, doi:10.1007/s00382-014-2056-1.

Bellomo, K., A. C. Clement, T. Mauritsen, G. Rädel, and B. Stevens (2015), The influence of cloud feedbacks on equatorial Atlantic variability, *J. Clim.*, *28*(7), 2725–2744, doi:10.1175/JCLI-D-14-00495.1.

Bingham, R. J., C. W. Hughes, V. Roussenov, and R. G. Williams (2007), Meridional coherence of the North Atlantic Meridional Overturning Circulation, *Geophys. Res. Lett.*, *34*, L23606, doi:10.1029/2007GL031731.

Booth, B. B. B., N. J. Dunstone, P. R. Halloran, T. Andrews, and N. Bellouin (2012), Aerosols implicated as a prime driver of twentieth-century North Atlantic climate variability, *Nature*, *484*(7393), 228–232, doi:10.1038/nature10946.

Brown, P. T., W. Li, L. Li, and Y. Ming (2014), Top-of-atmosphere radiative contribution to unforced decadal global temperature variability in climate models, *Geophys. Res. Lett.*, *41*, 5175–5183, doi:10.1002/2014GL060625.

Brown, P. T., W. Li, and S.-P. Xie (2015a), Regions of significant influence on unforced global mean surface air temperature variability in climate models, *J. Geophys. Res. Atmos.*, *120*, 480–494, doi:10.1002/2014JD022576.

Brown, P. T., W. Li, E. C. Cordero, and S. A. Mauget (2015b), Comparing the model-simulated global warming signal to observations using empirical estimates of unforced noise, *Sci. Rep.*, *5*, doi:10.1038/srep09957.

Brown, P. T., W. Li, J. H. Jiang, and H. Su (2016), Unforced surface air temperature variability and its contrasting relationship with the anomalous TOA energy flux at local and global spatial scales, *J. Clim.*, doi:10.1175/JCLI-D-15-0384.1.

Buckley, M. W., and J. Marshall (2016), Observations, inferences, and mechanisms of the Atlantic Meridional Overturning Circulation: A review, *Rev. Geophys.*, *54*, doi:10.1002/2015RG000493.

Chylek, P., J. D. Klett, G. Lesins, M. K. Dubey, and N. Hengartner (2014), The Atlantic Multidecadal Oscillation as a dominant factor of oceanic influence on climate, *Geophys. Res. Lett.*, *41*, 1689–1697, doi:10.1002/2014GL059274.

Clement, A., K. Bellomo, L. N. Murphy, M. A. Cane, T. Mauritsen, G. Rädel, and B. Stevens (2015), The Atlantic Multidecadal Oscillation without a role for ocean circulation, *Science*, *350*(6258), 320–324, doi:10.1126/science.aab3980.

Cleveland, W. S. (1979), Robust locally weighted regression and smoothing scatterplots, *J. Am. Stat. Assoc.*, *74*(368), 829–836, doi:10.1080/01621459.1979.10481038.

Cunningham, S. A., et al. (2007), Temporal variability of the Atlantic Meridional Overturning Circulation at 26.5°N, *Science*, *317*(5840), 935–938, doi:10.1126/science.1141304.

Delworth, T. L., and M. E. Mann (2000), Observed and simulated multidecadal variability in the Northern Hemisphere, *Clim. Dyn.*, *16*(9), 661–676, doi:10.1007/s003820000075.

Delworth, T. L., et al. (2006), GFDL's CM2 global coupled climate models. Part I: Formulation and simulation characteristics, *J. Clim.*, *19*(5), 643–674, doi:10.1175/JCLI3629.1.

Enfield, D. B., A. M. Mestas-Nuñez, and P. J. Trimble (2001), The Atlantic Multidecadal Oscillation and its relation to rainfall and river flows in the continental U.S., *Geophys. Res. Lett.*, *28*(10), 2077–2080, doi:10.1029/2000GL012745.

Evan, A. T., R. J. Allen, R. Bennartz, and D. J. Vimont (2012), The modification of sea surface temperature anomaly linear damping time scales by stratocumulus clouds, *J. Clim.*, *26*(11), 3619–3630, doi:10.1175/JCLI-D-12-00370.1.

Folland, C. K., T. N. Palmer, and D. E. Parker (1986), Sahel rainfall and worldwide sea temperatures, 1901-85, *Nature*, *320*(6063), 602–607, doi:10.1038/320602a0.

Goldenberg, S. B., C. W. Landsea, A. M. Mestas-Nuñez, and W. M. Gray (2001), The recent increase in Atlantic hurricane activity: Causes and implications, *Science*, *293*(5529), 474–479, doi:10.1126/science.1060040.
Gulev, S. K., M. Latif, N. Keenlyside, W. Park, and K. P. Koltermann (2013), North Atlantic Ocean control on surface heat flux on multidecadal timescales, *Nature*, *499*(7459), 464–467, doi:10.1038/nature12268.
Jungclaus, J. H., H. Haak, M. Latif, and U. Mikolajewicz (2005), Arctic–North Atlantic interactions and multidecadal variability of the meridional overturning circulation, *J. Clim.*, *18*(19), 4013–4031, doi:10.1175/JCLI3462.1.
Knight, J. R., R. J. Allan, C. K. Folland, M. Vellinga, and M. E. Mann (2005), A signature of persistent natural thermohaline circulation cycles in observed climate, *Geophys. Res. Lett.*, *32*, L20708, doi:10.1029/2005GL024233.
Knight, J. R., C. K. Folland, and A. A. Scaife (2006), Climate impacts of the Atlantic Multidecadal Oscillation, *Geophys. Res. Lett.*, *33*, L17706, doi:10.1029/2006GL026242.
Knutti, R., D. Masson, and A. Gettelman (2013), Climate model genealogy: Generation CMIP5 and how we got there, *Geophys. Res. Lett.*, *40*, 1194–1199, doi:10.1002/grl.50256.
Latif, M., and N. S. Keenlyside (2011), A perspective on decadal climate variability and predictability, *Deep Sea Re.Part II*, *58*(17–18), 1880–1894, doi:10.1016/j.dsr2.2010.10.066.
Latif, M., C. Böning, J. Willebrand, A. Biastoch, J. Dengg, N. Keenlyside, U. Schweckendiek, and G. Madec (2006), Is the thermohaline circulation changing?, *J. Clim.*, *19*(18), 4631–4637, doi:10.1175/JCLI3876.1.
Li, J., C. Sun, and F.-F. Jin (2013), NAO implicated as a predictor of Northern Hemisphere mean temperature multidecadal variability, *Geophys. Res. Lett.*, *40*, 5497–5502, doi:10.1002/2013GL057877.
Lozier, M. S. (2010), Deconstructing the conveyor belt, *Science*, *328*(5985), 1507–1511, doi:10.1126/science.1189250.
Lozier, M. S. (2012), Overturning in the North Atlantic, *Annu. Rev. Mar. Sci.*, *4*(1), 291–315, doi:10.1146/annurev-marine-120710-100740.
Lozier, M. S., V. Roussenov, M. S. C. Reed, and R. G. Williams (2010), Opposing decadal changes for the North Atlantic Meridional Overturning Circulation, *Nat. Geosci.*, *3*(10), 728–734, doi:10.1038/ngeo947.
Mahajan, S., R. Zhang, and T. L. Delworth (2011), Impact of the Atlantic Meridional Overturning Circulation (AMOC) on Arctic surface air temperature and sea ice variability, *J. Clim.*, *24*(24), 6573–6581, doi:10.1175/2011JCLI4002.1.
Martin, E. R., C. Thorncroft, and B. B. B. Booth (2014), The multidecadal Atlantic SST—Sahel rainfall teleconnection in CMIP5 simulations, *J. Clim.*, *27*(2), 784–806, doi:10.1175/JCLI-D-13-00242.1.
McCarthy, G. D., I. D. Haigh, J. J. M. Hirschi, J. P. Grist, and D. A. Smeed (2015), Ocean impact on decadal Atlantic climate variability revealed by sea-level observations, *Nature*, *521*(7553), 508–510, doi:10.1038/nature14491.
Medhaug, I., and T. Furevik (2011), North Atlantic 20th century multidecadal variability in coupled climate models: Sea surface temperature and ocean overturning circulation, *Ocean Sci.*, *7*(3), 389–404, doi:10.5194/os-7-389-2011.
Messié, M., and F. Chavez (2011), Global modes of sea surface temperature variability in relation to regional climate indices, *J. Clim.*, *24*(16), 4314–4331, doi:10.1175/2011JCLI3941.1.
Myers, T. A., and J. R. Norris (2013), Observational evidence that enhanced subsidence reduces subtropical marine boundary layer cloudiness, *J. Clim.*, *26*, 7507–7524, doi:10.1175/JCLI-D-12-00736.1.
O'Reilly, C. H., M. Huber, T. Woollings, and L. Zanna (2016), The signature of low-frequency oceanic forcing in the Atlantic Multidecadal Oscillation, *Geophys. Res. Lett.*, *43*, doi:10.1002/2016GL067925.
Ramanathan, V., R. D. Cess, E. F. Harrison, P. Minnis, B. R. Barkstrom, E. Ahmad, and D. Hartmann (1989), Cloud-radiative forcing and climate: Results from the Earth Radiation Budget Experiment, *Science*, *243*(4887), 57–63, doi:10.1126/science.243.4887.57.
Rayner, D., et al. (2011), Monitoring the Atlantic Meridional Overturning Circulation, *Deep Sea Res. Part II*, *58*(17–18), 1744–1753, doi:10.1016/j.dsr2.2010.10.056.
Schlesinger, M. E., and N. Ramankutty (1994), An oscillation in the global climate system of period 65–70 years, *Nature*, *367*(6465), 723–726, doi:10.1038/367723a0.
Soden, B. J., A. J. Broccoli, and R. S. Hemler (2004), On the use of cloud forcing to estimate cloud feedback, *J. Clim.*, *17*(19), 3661–3665, doi:10.1175/1520-0442(2004)017<3661:OTUOCF>2.0.CO;2.
Sun, C., J. Li, and F.-F. Jin (2015), A delayed oscillator model for the quasi-periodic multidecadal variability of the NAO, *Clim. Dyn.*, *45*(7), 2083–2099, doi:10.1007/s00382-014-2459-z.
Sutton, R. T., and D. L. R. Hodson (2005), Atlantic Ocean forcing of North American and European summer climate, *Science*, *309*(5731), 115–118, doi:10.1126/science.1109496.
Taylor, K. E., R. J. Stouffer, and G. A. Meehl (2011), An overview of CMIP5 and the experiment design, *Bull. Am. Meteorol. Soc.*, *93*(4), 485–498, doi:10.1175/BAMS-D-11-00094.1.
Ting, M., Y. Kushnir, R. Seager, and C. Li (2009), Forced and internal twentieth-century SST trends in the North Atlantic*, *J. Clim.*, *22*(6), 1469–1481, doi:10.1175/2008JCLI2561.1.
Trenberth, K. E., J. T. Fasullo, and J. Kiehl (2009), Earth's global energy budget, *Bull. Am. Meteorol. Soc.*, *90*(3), 311–323, doi:10.1175/2008BAMS2634.1.
von Storch, H., and S. W. Zwiers (2003), *Statistical Analysis in Climate Research*, Cambridge Univ. Press, Cambridge, U. K.
Wang, C., S. Dong, A. T. Evan, G. R. Foltz, and S.-K. Lee (2012), Multidecadal covariability of North Atlantic sea surface temperature, African dust, Sahel rainfall, and Atlantic hurricanes, *J. Clim.*, *25*(15), 5404–5415, doi:10.1175/JCLI-D-11-00413.1.
Xie, S.-P., and S. G. H. Philander (1994), A coupled ocean-atmosphere model of relevance to the ITCZ in the eastern Pacific, *Tellus A*, *46*(4), 340–350, doi:10.1034/j.1600-0870.1994.t01-1-00001.x.
Yuan, T., L. Oreopoulos, M. Zelinka, H. Yu, J. Norris, M. Chin, S. Platnick, and K. Meyer (2016), Positive low cloud and dust feedbacks amplify tropical North Atlantic Multidecadal Oscillation, *Geophys. Res. Lett.*, *43*, 1349–1356, doi:10.1002/2016GL067679.
Zhang, J., and R. Zhang (2015), On the evolution of Atlantic Meridional Overturning Circulation fingerprint and implications for decadal predictability in the North Atlantic, *Geophys. Res. Lett.*, *42*, 5419–5426, doi:10.1002/2015GL064596.
Zhang, R. (2015), Mechanisms for low-frequency variability of summer Arctic sea ice extent, *Proc. Natl. Acad. Sci. U.S.A.*, *112*(15), 4570–4575, doi:10.1073/pnas.1422296112.
Zhang, R., and T. L. Delworth (2006), Impact of Atlantic Multidecadal Oscillations on India/Sahel rainfall and Atlantic hurricanes, *Geophys. Res. Lett.*, *33*, L17712, doi:10.1029/2006GL026267.
Zhang, R., S. M. Kang, and I. M. Held (2010), Sensitivity of climate change induced by the weakening of the Atlantic Meridional Overturning Circulation to cloud feedback, *J. Clim.*, *23*(2), 378–389, doi:10.1175/2009JCLI3118.1.
Zhang, R., et al. (2013), Have aerosols caused the observed Atlantic multidecadal variability?, *J. Atmos. Sci.*, *70*(4), 1135–1144, doi:10.1175/JAS-D-12-0331.1.